

## Experimental verification on the robustness and stability of an interaction control: Single-degree-of-freedom robot case

Sang Hyun Park,<sup>1,2</sup> Jeongwoo Son,<sup>1</sup> Maolin Jin,<sup>2</sup> and Sang Hoon Kang<sup>1</sup>, 

<sup>1</sup>Mechanical Engineering Department, Ulsan National Institute of Science and Technology, Ulsan, Republic of Korea

<sup>2</sup>Human-Centered Robotics Research Center, Korea Institute of Robotics and Technology Convergence (KIRO), Pohang, Republic of Korea

✉ Email: sanghokang@unist.ac.kr

The nonlinear bang-bang impact control (NBBIC) had been proposed for robots performing tasks having frequent contact with different environments because it takes advantage of the frictions in robot joints that are not helpful for constrained space control usually, does not need to change gains throughout tasks, and requires little information on robot dynamics. Despite these advantages, due to the lack of stability proof, it was not widely adopted. Recently, the stability of the NBBIC for one degree-of-freedom (DOF) robot has been proved almost two decades after its first proposal. The stability condition provided a theoretical stable region of the inertia estimate and was not dependent on environment dynamics, indicating the robustness of NBBIC to environment dynamics (e.g. stiffness). Thus, there is a strong need to verify the stability condition and the robustness of NBBIC to environment dynamics. Experiments of single DOF robots colliding with various environments showed that the stability condition predicted the stable range of the inertia estimate well, though there was a reduction in upper-bound because of sensor noise. The impact force response did not vary significantly for environments with different stiffness (silicon, aluminium, and steel wall), thereby confirming the robustness of the NBBIC to environment dynamics.

**Introduction:** Many robots need to make frequent physical interactions (e.g. contacts) with environments, humans, and other robots to successfully execute assigned jobs, including rehabilitation, space exploration, and many industrial applications. Those frequent interactions may include an impact between a robot and an environment in transitioning from free-space to constrained-space. For the successful execution of those tasks, the robot control law needs to effectively deal with the un-modelled/unknown dynamics, unexpected disturbances, and rapidly changing environment conditions, including the environment stiffness and the consequent abrupt changes in the external forces. Moreover, it is preferable for practical implementation that the control law is independent of the robot and environment models. The nonlinear bang-bang impact control (NBBIC) was able to deal with such tasks without changing gains and without using a robot and environment dynamics [1, 2]. Moreover, to absorb the impact force and energy at the sudden contact with an unknown environment, the controller takes advantage of the nonlinear joint frictions, which are usually known to degrade the control performance [1, 2]. The controller needs the most recent acceleration and joint torque to compensate for the uncertain robot dynamics instead of the robot dynamics model [3–5], which has inevitable modelling error. Thus, the controller was simple, and its implementation was straightforward. A study comparing the NBBIC with other impact controllers showed its superior performance through one degree-of-freedom (DOF) robot experiments [1]. However, only recently (almost 20 years after its first proposal), its stability was formally proved by the authors [2] for one DOF robot due to the difficulty of tackling the highly nonlinear complicated impact situations. In [2], the stability condition predicted that the controller is robust to environment changes (e.g. stiffness) and disturbances, and the nonlinear joint frictions are indeed helpful for the stabilization of the robot experiencing a rapidly changing impact force due to sudden impact to an extremely stiff environment at very high velocity. Thus, it is necessary to verify the prediction from the stability analysis experimentally, though the analysis was rigorous. The verification would confirm that, under the non-ideal conditions that do not guarantee the direct measurement of all the necessary joint kinematic variables and contact force with infinite precision, the controller can be

practically used for the tasks with many intended/unintended contacts with different environments. Moreover, it will also inspire researchers to develop advanced control schemes that make smarter use of joint friction to handle tasks that require robots to be in frequent contact with various environments. In this paper, with a single DOF robot and different environments, the controller stability proof given in [2] was, thus, experimentally verified for the first time.

**Nonlinear bang-bang impact control:** The nonlinear dynamics of one DOF has the following form:

$$\tau(t) = M\ddot{\theta}(t) + G(\theta(t)) + \tau_s(t) + d(t), \quad (1)$$

where  $M$  indicates inertia;  $G$  gravitational force;  $\theta$ ,  $\dot{\theta}$  joint angle and its time derivatives;  $\tau$  joint torque;  $\tau_s$  external torque;  $d$  represents nonlinear joint frictions and unknown disturbances. The robot dynamics can be rewritten by introducing  $\bar{M}$ , a constant inertia estimate, as follows:

$$\tau(t) = \bar{M}\ddot{\theta}(t) + H(t), \quad (2)$$

where

$$H(t) = (M - \bar{M})\ddot{\theta} + G(\theta) + d + \tau_s. \quad (3)$$

The natural admittance control combined with the robust and model-independent time delay control (NAC/TDC) was proposed as [1, 2]:

$$\tau(t) = \bar{M}u(t) - \bar{M}\ddot{\theta}(t - L) + \tau(t - L), \quad (4)$$

where,

$$u(t) = K_d e(t) + B_d \dot{e}(t) + G_v [\dot{\theta}_{cmd}(t) - \dot{\theta}(t)] + c_r \theta(t), \quad (5)$$

$$\dot{\theta}_{cmd}(t) = \int [\tau_s + K_d e(t) + B_d \dot{e}(t)] M_s^{-1} dt, \quad (6)$$

$$e(t) = \theta_d(t) - \theta(t), \quad (7)$$

and  $K_d$  denotes the desired stiffness;  $B_d$  desired damping coefficient;  $M_s$  end-point mass;  $G_v$  a constant velocity feedback gain;  $L$  the intentional time-delay that, in many cases, is designated to be the sampling time;  $\theta_d$  and  $\dot{\theta}_d$  reference trajectory and its derivative, respectively;  $\dot{\theta}_{cmd}$  command joint velocity; and  $c_r$  stands for a constant introduced for the enhancement of system stability. If  $L$  is sufficiently small [6], the time-delay estimation (TDE) term ( $\hat{H}(t) = -\bar{M}\ddot{\theta}(t - L) + \tau(t - L)$ ), which is the estimate of the environment and robot dynamics  $H(t)$  and used to compensate for  $H(t)$ , accurately estimate the dynamics instead of using the robot and environment dynamics equations, because  $\hat{H}(t)$  is  $H(t - L)$  [1, 2, 6, 7]. Consequently, the TDE error,  $\varepsilon(t) (\triangleq \bar{M}^{-1}[H(t) - \hat{H}(t)])$  [2], representing the difference between the real dynamics and the estimated dynamics, becomes zero as  $L$  goes to zero [1, 2, 6, 7]. The NBBIC strategy, based on the NAC/TDC, was given below [1, 2].

1. Unconstrained motion ( $|F_s| < F_{impact}$ ): NAC/TDC.
2. In contact transition: bang-bang control
  - a. In contact with an environment ( $|F_s| > F_{sw}$ ): NAC/TDC.
  - b. Out of contact ( $|F_s| < F_{sw}$ ):  $\tau(t) = 0$ .
  - c. Stopped ( $|F_s| < F_{sw}$  &  $|\dot{\theta}(t)| < \dot{\theta}_{threshold}$ ): NAC/TDC.
3. After impact transient ( $|F_s| > F_{sw}$ ): NAC/TDC.

Here  $F_s$  denotes measured external force;  $F_{impact}$ ,  $F_{sw}$ , and  $\dot{\theta}_{threshold}$  represent non-zero threshold values to determine impact and contact with an environment, and movement with respect to the environment, respectively, and the noise level and resolution of the sensors determine the threshold values [1, 2]. For free-space and constrained motions, one uses NAC/TDC. For the transition, if the contact of the robot with an environment is lost due to the large and abrupt impact force, control torque becomes zero, and the impact energy is absorbed by joint frictions. In short, NBBIC does not need an environment model or robot dynamics

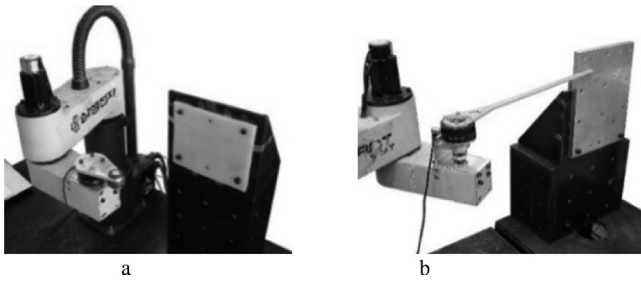


**Fig 1** Experimental set up. (a) Stability verification set up. (b) Robustness test set up (a long aluminium link at the end of SCARA)

model, and joint friction is sensibly utilized to make the robot stably contacting with an environment. The NBBIC for multi-DOF robots is given in [8, 9]. These points became evident with the rigorous stability analysis [2].

*NBBIC Stability Theorem [2]*: The sufficient stability condition for a one DOF robot under NBBIC is

$$\| \|1 - M^{-1}\bar{M}\|_{12}\|_{\infty} < (1 - c)/1 + (\beta_4\kappa_1 + \beta_5\kappa_2 + \beta_6\kappa_3), \quad (8)$$

where

$$\begin{aligned} \kappa_1 &= \|G_v M_s^{-1} K_d\|_{12}, \kappa_2 = \|G_v M_s^{-1} B_d + K_d - c_r\|_{12}, \kappa_3 = \|G_v + B_d\|_{12} \\ c &= \beta_4 \|M^{-1} q_2(t)\|_{12}\|_{\infty} + \beta_5 \|M^{-1} q_1(t)\|_{12}\|_{\infty} + \beta_1 \|M^{-1} \tilde{q}_2(t)\|_{12}\|_{\infty} \\ &+ \beta_2 \|M^{-1} \tilde{q}_1(t)\|_{12}\|_{\infty} \end{aligned} \quad (9)$$

$\tilde{\bullet}$  denotes  $\bullet(t) - \bullet(t-L)$ ;  $\beta_i$  represents  $L_{\infty}$  gains of operator  $H_i$  ( $i = 1, 2, \dots, 5$ ), respectively, where  $H_i$ s represent operators as  $H_1: \varepsilon \mapsto e$ ,  $H_2: \varepsilon \mapsto \dot{e}$ ,  $H_3: \varepsilon \mapsto \tilde{e}_1$ ,  $H_4: \varepsilon \mapsto \tilde{e}$ , and  $H_5: \varepsilon \mapsto \tilde{e}$ ;  $e_l$  time integration of  $e$ ;  $q_1(t)$  and  $q_2(t)$  are bounded terms that are dependent on  $\dot{e}$  and  $e$ , respectively, and are used to represent the friction and bounded disturbance effects [2].  $c$  in (13) consists of  $\beta_4$  and  $\beta_5$  (small values that are obtained by integrating the difference of stable linear systems' impulse responses through time), multiplied by  $\tilde{q}_1$  and  $\tilde{q}_2$  (the differences between the current time and a recent past-time bounded values). Thus,  $c$  can be neglected during the transition and the constrained motion, during which velocity and position change negligibly within a small-time step  $L$  [2, 10]. From the stability condition, it was found that if NBBIC is stable during unconstrained motion in free-space, it is also stable during the constrained motion. Moreover, because the stability condition does not need environment dynamics, which is usually vital information to guarantee the stability of an interaction controller, the NBBIC is robust to environment changes [2]. The stability analysis indicates that the nonlinear bang-bang action's effectiveness relies only on frictions if NAC/TDC was tuned to be stable [2]. Note, however, that if a robot has low friction, providing gravity compensation may be a good strategy in case 2-b. In other words, the zero control input in (10) could be replaced with gravitational torque, if needed. In [2], the stability condition had been, first, verified with extensive simulations under ideal conditions that all the kinematic variables are known with infinite precision without any noise [2]. Thus, experimental verification is strongly needed. Note that the tuning of controller design parameters  $\bar{M}$ ,  $G_v$ , and  $c_r$  can be found in [2].

*Experiments*: For the verification of stability condition, the second link of the Selective Compliance Assembly Robot Arm (SCARA) was used with the first (base) joint locked. The second link was 0.1865 m long, weighed 6.82 kg, and has an inertia of 0.224 kg·m<sup>2</sup>. At joint 2, a brushless DC motor (0.92Nm stall torque) was connected to a gear (gear reduction ratio: 80:1) having Coulomb friction of 3 Nm, and the rotation of the motor was measured using a resolver (resolution: 4096 pulses/rev) attached to the shaft. At the end of the robot, a force sensor (ATI Gamma SI-130-10, 10Nm range) was attached (Figure 1a). For the test of the robustness of the NBBIC to environment changes and disturbances, a rigid 0.5 m aluminium link was installed at the end of the second link of the SCARA to achieve the highest impact velocity within the force sensor range (Figure 1b). Only the aluminium link was used while the robot motors are locked. A DC motor with a 0.18° resolution encoder

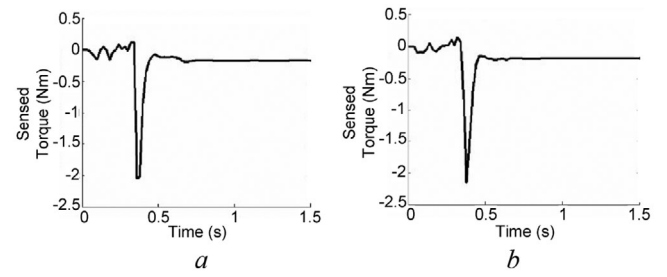


**Fig 2** Contact force response. (a)  $\bar{M} = 0.0284 \text{ kg}\cdot\text{m}^2$  (experimentally obtained lower bound). (b)  $\bar{M} = 0.036 \text{ kg}\cdot\text{m}^2$  (experimentally obtained upper bound)

was connected to a 26:1 planetary gear, which was, in turn, connected to the force sensor that was firmly connected to the aluminium link. The sampling time and time delay  $L$  were both 1 ms. Backward Euler differentiation was used to obtain joint angular velocity and acceleration [7]. Thus, there were significant noises due to quantization errors in joint angle, angular velocity, angular acceleration, and force. The controller was implemented in a real-time operating system, QNX.

*Stability verification*: The task was to start the robot in free-space and travel a distance of 0.0746 m at a desired constant speed of 0.1865 m/s.  $\theta_d$  was a ramp and hold function of time with the slope of 1 rad/s for the first 0.4 s. In reality, the robot travelled 0.0728 m in free-space and contacted the Si wall with a transition in between. The stability theorem provided a stable range of  $\bar{M}$  was  $0.0284 \text{ kg}\cdot\text{m}^2 \leq \bar{M} \leq 0.371 \text{ kg}\cdot\text{m}^2$  for setting  $G_v$  as 12 N·m/s,  $B_d$  as 30 N·m/s,  $K_d$  as 140 Nm, and  $M_s$  as 0.12 kg·m<sup>2</sup>. The robot was stable with the lower bound value from the stability condition (Figure 2a). However, 0.036 kg·m<sup>2</sup> was the experimental stable upper bound of  $\bar{M}$  (Figure 2b).

The noises may further restrict experimental stable upper bound in velocity and acceleration signals. If we adopt a discrete-time first-order low-pass filter to attenuate noise, NAC/TDC control input becomes [11]

$$\tau'(t) = \bar{M} [u(t) - \ddot{\theta}(t-L)] + \tau(t-L), \quad (10)$$

$$\tau(t) = (\lambda'/1 + \lambda') \tau'(t) + (1/1 + \lambda') \tau(t-L) \quad (\lambda' = \lambda L), \quad (11)$$

where  $\lambda$  denotes the cut-off frequency of the low-pass filter;  $\tau'$  represents the NAC/TDC's control input before filtering; and  $\tau$  stands for the low-pass filtered control input. Substituting (15) into (16) yields

$$\tau(t) = (\lambda'/1 + \lambda') \bar{M} [u(t) - \ddot{\theta}(t-L)] + \tau(t-L). \quad (12)$$

Thus, the use of reduced  $\bar{M}$  is equivalent to low-pass filtering the control input. This explains the difference between the stable upper bound of  $\bar{M}$  obtained from experiments and the stability analysis. For the attenuation of the noise, the upper bound of  $\bar{M}$  guaranteeing stability became smaller than the one predicted by the stability analysis. We found that  $\lambda = 107.5 \text{ rad/s}$  is the cut-off frequency of the first order low-pass filter that can reduce the theoretical upper bound of  $\bar{M}$  down to the experimentally found upper bound.

*Robustness to environment dynamics*: During the task for this experiment, the robot first moved in free-space, impacted to various environments (silicon, aluminium, and steel walls) with a fast 1.5 m/s velocity, and moved in constrained space while making a stable contact with the environment (Figure 3).  $\theta_d$  was a ramp and hold function of time with the slope of 3 rad/s for the first 0.4 s. The aluminium link (Figure 1b) was used for this experiment. The robot with the control gains, tuned to for the best performance in contact transition with aluminium wall and satisfied the stability condition, hit various environments at a 1.5 m/s velocity and experienced  $\sim 4.5 \text{ Nm}$  impact force with 0.25 s settling time. The same gains were used for the walls. The performance measure for this experiment was the settling time of the force response [1]. For the soft silicon wall (Figure 3b), the contact force response, especially the

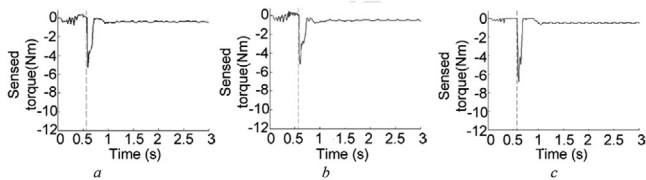


**Fig 3** Force responses (dashed line: impact time). (a) Impact to an Al wall. (b) Impact to a Si wall. (c) Impact to a steel wall

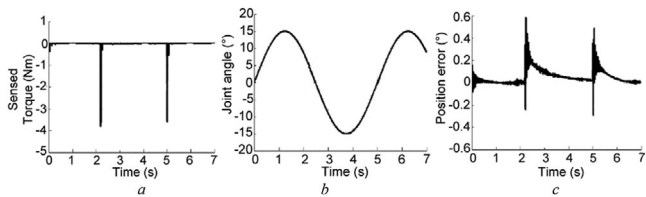


**Fig 4** Disturbance rejection in free space. (a) Disturbance torques. (b) Robot position under NBBIC. (c) Position error

settling time, was not much different from that with a stiff steel wall (Figure 3c). Thus, these results prove that NBBIC is robust to environment dynamics, including stiffness, indicating its high potential for tasks in unknown/un-modelled environments. It was observed that the impact force response was depending on the operating conditions, including humidity and temperature that affect the friction in the robot joint.

**Robustness to pulse disturbances:** The free-space disturbance rejection performance of NBBIC was tested with the same gains used to verify the robustness to environment dynamics. We manually hit the robot by using an aluminium stick with a sudden torque of  $\sim 3.5$  Nm (Figure 4a) while the robot was following a sinusoidal trajectory (Figure 4b). The robot followed the desired trajectory successfully with a small increase in position error (Figure 4c), the performance measure, despite the pulse disturbances, indicating the NBBIC is robust to disturbances while accomplishing free-space tasks.

The experimental results demonstrate that the NBBIC effectively subsides impact oscillations, constrained motion, and trajectory following despite sudden disturbances, all with one set of control gains. In other words, the stability was properly analysed, and the stability condition predicted the aforementioned properties of NBBIC successfully.

**Conclusion:** The theoretical results of the stability analysis were verified experimentally. The NBBIC was robust to disturbances and environments. The nonlinear joint friction helped to stabilise the sudden contact with various environments. Without changing algorithms and gains, free-space motion, transition, and constrained motion could be dealt with NBBIC. Changes in environment stiffness did not affect control performances. All these results indicate that the predictions made with the stability analysis are plausible. In other words, a difficult problem, which was left unsolved for almost 20 years, was eventually proved with substantial experimental evidence. Moreover, interestingly, the nonlinear friction indeed helped stabilize the robot experiencing sudden

impact force with a stiff environment at a fast velocity as predicted by the stability analysis, indicating a potential beneficial use of the nonlinear joint friction for robot tasks having frequent interaction with various environments. From now on, one can confidently use the NBBIC with the strong theoretical proof that is verified with extensive experimental studies. Further studies on a stability analysis of a multi-DOF robot case and its experimental validation are warranted to generalize the results and facilitate the use of the controller for multi-DOF robots.

**ACKNOWLEDGEMENTS:** This work was supported in part by Basic Science Research Program through the National Research Foundation of Korea (NRF) funded by the Ministry of Education (2018R1D1A1B07049862) and in part by Korea Electric Power Corporation (Grant number: R20X002-5).

© 2021 The Authors. *Electronics Letters* published by John Wiley & Sons Ltd on behalf of The Institution of Engineering and Technology

This is an open access article under the terms of the Creative Commons Attribution License, which permits use, distribution and reproduction in any medium, provided the original work is properly cited.

Received: 25 November 2020 Accepted: 4 March 2020

doi: 10.1049/el12.12151

## REFERENCES

- Lee, E., et al.: Bang-bang impact control using hybrid impedance/time-delay control. *IEEE/ASME Trans. Mechatronics* **8**(2), 272–277 (2003)
- Kang, H., Lee, S.J., Kang, S.H.: Stability of a robust interaction control for single-degree-of-freedom robots with unstructured environments. *Intel. Serv. Robot.* **13**(3), 393–401 (2020)
- Yu, X., et al.: Adaptive fuzzy full-state and output-feedback control for uncertain robots with output constraint. *IEEE Trans. Syst., Man, Cybern. Syst.* (2020). <https://doi.org/10.1109/TSMC.2019.2963072>
- He, W., et al.: Dynamical modeling and boundary vibration control of a rigid-flexible wing system. *IEEE ASME Trans. Mechatronics* **25**(6), 2711–2721 (2020)
- He, W., et al.: Modeling and trajectory tracking control for flapping-wing micro aerial vehicles. *IEEE/CAA J. Autom. Sin.* **8**(1), 148–156 (2021)
- Youcef-Toumi, K., Ito, O.: A time delay controller for systems with unknown dynamics. *ASME J. Dyn. Syst. Meas. Control* **112**(1), 133–142 (1990)
- Hsia, T.C., Gao, L.S.: Robot manipulator control using decentralized linear time-invariant time-delayed joint controllers. In: Proc. of the 2005 IEEE Int. Conf. on Robotics and Automation, pp. 2070–2075. IEEE, Piscataway, NJ (1990)
- Jin, M., et al.: Nonlinear bang-bang impact control: A seamless control in all contact modes. In: Proc. of the 2005 IEEE Int. Conf. on Robotics and Automation, pp. 557–564. IEEE, Piscataway, NJ (2005)
- Kang, S.H., et al.: Nonlinear bang-bang impact control for free space, impact and constrained motion: Multi-dof case. In: Proc. of the 2005, American Control Conf., pp. 1913–1920. IEEE, Piscataway, NJ (2005)
- Pagilla, P.R., Biao, Y.: A stable transition controller for constrained robots. *IEEE/ASME Trans. Mechatronics* **6**(1), 65–74 (2001)
- Youcef-Toumi, K., Wu, S.-T.: Input/output linearization using time delay control. *ASME J. Dyn. Syst. Meas. Control* **114**(1), 10–19 (1992)